Journal of Petroleum Exploration and Production Technology
https://doi.org/10.1007/s13202-024-01863-y

ORIGINAL PAPER - PRODUCTION ENGINEERING

Weighted mapping of productivity potential based on simulated annealing algorithm for well placement optimization

Rui Deng[1] · Bo Kang[1,2] · Liang Zhang[1] · Lian Wang[1] · Bing Xu[1] · Xing Zhao[1] · Ce Duan[1]

Received: 30 May 2024 / Accepted: 10 August 2024

Abstract

In the realm of reservoir development, the optimization of well placement constitutes a cornerstone challenge with significant implications that directly determine the recovery rate and economic benefits of oil and gas production. This research proposes a novel approach to optimizing well placement in reservoirs by integrating reservoir numerical simulations with intelligent optimization algorithms. The quintessence of this inquiry revolves around the strategic placing of wells amidst the complex geological fabric of reservoirs, where the objective function landscape often manifests with non-smooth, multimodal characteristics. To address those issues, the Weighted Mapping of Productivity Potential (WMPP) technique, fortified by the Simulated Annealing algorithm to judiciously ascertain specific weighting coefficients for the computation of WMPP across reservoirs is introduced in this study. Furthermore, an emblematic carbonate reservoir model serves to corroborate the adaptability and viability of WMPP for well placement optimization, underscoring its efficacy as a swift, economically viable instrument for the delineation of prospective reservoir zones and the guidance of drilling initiatives. The optimization results show that the well placement scheme guided by WMPP, which required 7 fewer wells than the oil initially in place (OOIP)-based scheme, improved 21.74% oil production over the twenty years production period. This comprehensive workflow proffers invaluable insights and benchmarks for the formulation of well placement strategies, with the proposed methodology, in its apparent simplicity, showcasing remarkable efficiency.

Keywords Well placement optimization · Productivity potential · Simulated annealing algorithm · Middle Eastern carbonate reservoir

Abbreviations

DMPP	Direct mapping of productivity potential
MMSTB	Million stock tank barrels
mD	Mini darcy
OOIP	Oil initially in place
PINDEX_OPT	The optimized potential index by WMPP method
SA	Simulated annealing
SPSA	Simultaneous perturbation stochastic Approximation
WMPP	Weighted mapping of productivity potential
WOPT	Well oil total production
FTOP	Filed total oil production

List of symbols

$\mathrm{cov}(\cdot)$	Standard covariance
$d_{goc,i,j,k}$	The distance from the grid block (i,j,k) to the closest gas-oil interface
$d_{woc,i,j,k}$	The distance from the grid block (i,j,k) to the closest oil–water interface
ΔE	The change in the objective function between the current solution and new solution
g	The grid block index, i.e. (i,j,k)
$g_{w,N}$	The total number of grids of in the well cut of well w
$g_{w,n}$	The grid numbered n within the well cut of well w
$I_{i,j,k}(t)$	The WMPP at position (i,j,k) at time t
$J_{i,j,k}(t)$	The DMPP at gird block (i,j,k) at time t
$K_{i,j,k}$	The permeability at gird block (i,j,k)
P_{accept}	The probability of accepting the new solution
p_{min}	The minimum well bottomhole pressure

✉ Liang Zhang
zhangliang@zhenhuaoil.com

[1] Chengdu North Petroleum Exploration and Development Technology Co., Ltd., Chengdu, Sichuan Province, China

[2] EBS PETROLEUM Co., Ltd., Baghdad, Iraq

Published online: 20 August 2024

$p_{o,i,j,k}(t)$	The oil pressure at gird block (i,j,k) at time t
$r_{i,j,k}$	The distance from the gird block (i,j,k) to the closest boundary
$S_{o,i,j,k}(t)$	The oil saturation at gird block (i,j,k) at time t
S_{or}	The residual saturation of oil at gird block (i,j,k)
T_{new}	The new temperature
T_{old}	The current temperature
x	The original value of data
$\phi_{i,j,k}$	The porosity at the grid block (i,j,k)
ρ	The spearman rank correlation coefficient
$\sigma(\cdot)$	Standard deviation
ω	A row vector of weights of corresponding variables
ω^*	The most optimized ω that maximizes the Spearman coefficient between WMPP and WPT of wells
$\Delta\omega_m$	The small change in solution of a specific weight numbered m in ω
$\omega_{new,m}$	The new solution in solution of a specific weight numbered m in ω
$\omega_{old,m}$	The current solution in solution of a specific weight numbered m in ω

Introduction

Optimization of well placement is an essential procedure in close-loop reservoir management. Traditional methods for determining well placement have predominantly comprised analytical approaches rooted in reservoir engineering and reservoir mechanics theories, along with semi-empirical techniques guided by numerical simulations and empirical insights (Olabode et al. 2021; Wang et al. 2023; Rostamian et al. 2024). Analytical methods seek to establish relationships between objective functions, such as breakthrough time and sweep efficiency, for diverse well configurations and subsequently maximize these functions to identify the optimal well placement strategy (Syed et al., 2021). Notable methodologies encompass the equivalent permeability resistance method, vector well pattern method, and conformal transformation method (Lang et al. 1993; Liu et al. 2005). Conversely, semi-empirical methods are predominantly guided by pragmatic considerations, particularly the actual distribution of oil saturation within the reservoir. These methods involve formulating multiple well placement schemes based on empirical knowledge, followed by a comparative analysis conducted through reservoir numerical simulations to identify the most favorable well placement configuration. However, it is important to note that such methods possess limited flexibility for comparative analysis, are susceptible to significant subjective influence, and frequently face challenges in achieving the truly optimal solution (Ji et al. 1994; Ling et al. 2007; Chen et al. 2009).

Advancements in computer technology and the emergence of intelligent oilfield technology have paved the way for integrating optimization theory with reservoir numerical simulation techniques (Azamipour et al. 2023). This integration has abstracted well placement design as a mathematical optimization problem, transforming the complex engineering challenge of optimizing well deployment in reservoirs into a feasible endeavor (Humphries et al., 2015; Sobhi et al. 2022). Guyaguler (2002) pioneered the combination of genetic algorithms with polytope methods, surrogate models, and other techniques to develop a hybrid genetic algorithm for solving well placement optimization problems. Building on this approach, Badru and Kabie (2003) also employed a hybrid genetic algorithm to optimize well placement and trajectories, particularly for horizontal wells. Yeten et al. (2003) adopted a novel approach by utilizing a hybrid genetic algorithm that incorporated hill climbing algorithms, artificial neural networks, and near-well coarsening techniques to optimize well type, placement, and trajectories in unconventional reservoirs. Bouzarkouna et al. (2012) introduced an adaptive covariance matrix evolutionary algorithm coupled with a surrogate model for optimizing well placement and trajectories, with a specific focus on horizontal wells. Bellout and Volkov (2018) successfully integrated reservoir engineering expertise with sequential quadratic programming and differential evolution to address real-world nonlinear constraints, effectively reducing the search space for optimization variables—an essential aspect of optimizing large-scale reservoir numerical simulations. Bangerth et al. (2006) harnessed the Simultaneous Perturbation Stochastic Approximation (SPSA) algorithm for optimal well placement design. They conducted a comparative analysis, pitting SPSA against finite difference gradient methods and fast simulated annealing algorithms in a 7-well placement problem, demonstrating SPSA's robustness and superior optimization efficiency. Leeuwenburgh et al. (2010) leveraged ensemble-based optimization methods for well placement in two distinct reservoir models, involving the placement of 9 wells—comprising 3 injection wells and 6 production wells.

The outcomes of the aforementioned research have significantly enhanced sweep efficiency and net present value compared to the original designs. The iterative calculations of optimization algorithms to determine optimal well deployment often necessitate hundreds or even thousands of calls to reservoir numerical simulations (Wang et al. 2023). This substantial computational resource consumption poses a challenge in swiftly solving the high-dimensional optimization problem associated with well placement in reservoirs. In response to this challenge, surrogate modeling techniques

have gained widespread attention in recent years. These techniques involve constructing computationally efficient approximations for large-scale systems, relying on a limited set of sample information while preserving computational accuracy (Algosayir 2012; Thenon et al. 2016; Ghassemzadeh et al. 2019; Shahk et al. 2020; Wang et al. 2021).

When employing the streamline model (Portella and Hewett 2000; Heijn et al., 2004; Wang et al. 2022) as a simplified reservoir numerical simulation model, it utilizes a network of streamlines to emulate multiphase displacement in porous media. Each streamline is treated as a one-dimensional system, and the Buckley-Leverett equation is resolved along the streamline. However, the streamline paths in this model remain fixed and do not readily accommodate reservoir heterogeneity and other intricacies, thereby imposing limitations on accuracy. Akin et al. (2010) addressed this challenge by developing a variety of neural network surrogate models tailored to reservoir numerical simulation. These surrogate models were subsequently integrated with optimization algorithms to facilitate the achievement of optimal well placement in reservoirs. However, when dealing with a substantial number of wells in the context of reservoir well placement, the 'curse of dimensionality' pertaining to optimization variables during surrogate model construction and optimization algorithm iterations can lead to extended computation times and diminished surrogate accuracy. Liu and Jalali (2006) introduced a formula for calculating reservoir production potential grounded in principles of mass balance, Darcy's law, and real-world production constraints. The formula incorporates parameters such as oil saturation, oil-phase pressure, and absolute permeability. Ding et al. (2014) took into account the principal factors influencing well production and introduced the concept of the direct mapping of productivity potential (DMPP). DMPP serves as a representation of regions within the reservoir area characterized by varying production potential. It aids optimization algorithms in identifying relatively high-value areas during initial iterations. However, it's important to note that DMPP may not be ideally suited for optimizing well placement designs in diverse types of reservoirs.

To address this issue, this paper will build upon DMPP and combine it with the Simulated Annealing optimization algorithm to develop a production potential index calculation method that can be applied to various types of reservoirs. By using a set of specific weighting coefficients, we will obtain the Weighted Mapping of Productivity Potential (WMPP) for the particular reservoir. WMPP will serve as a guidance tool for reservoir well placement, facilitating more effective deployment strategies. This innovative approach will consider critical factors such as porosity, permeability, pressure, and fluid properties, integrating geological and engineering data to ensure accurate representation. The combination of WMPP and Simulated Annealing aims to optimize well placement by maximizing overall production potential while considering operational constraints and economic factors, thereby enhancing recovery rates and improving reservoir management.

Model description

The H-3B reservoir model represents a real-world Middle Eastern porous carbonate reservoir. This reservoir model is a three-phase, three-dimensional reservoir simulation model. It comprises 100 simulation layers with constant thickness and is geologically bounded by a fault to the east and south. The model encompasses a total of $973 \times 397 \times 100$ grid blocks, with each grid block measuring 50 m in the x and y directions, and 1 m in the z direction. Among these grid blocks, 3,080,200 are active. The porosity and permeability fields is illustrated in Fig. 1, where the average porosity is

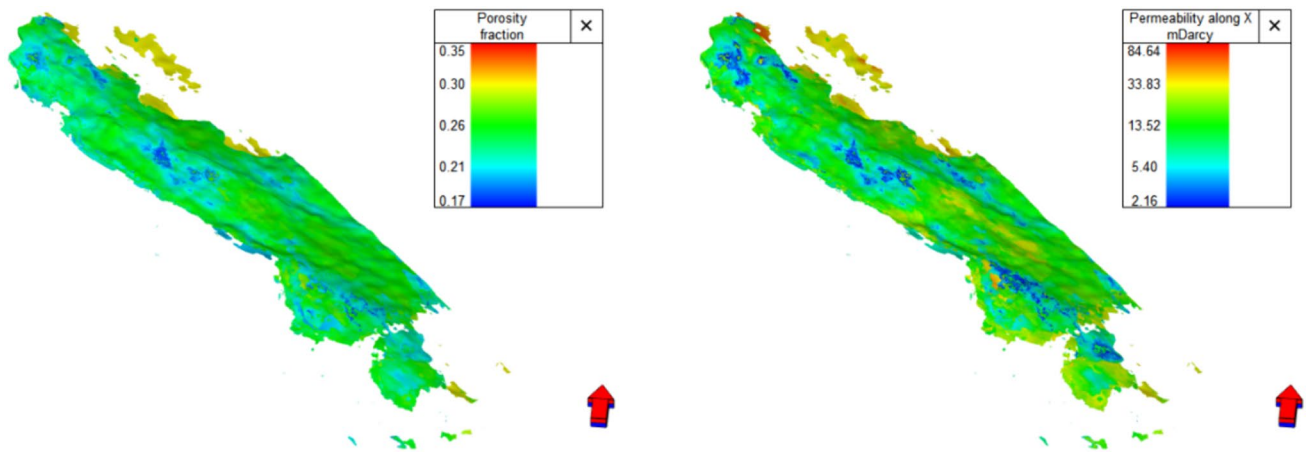

Fig. 1 The porosity (lift) and permeability (right) field of the H-3B reservoir (the red arrow points in the direction of north)

0.25, and the permeability averages 19 mD. Notably, the model does not incorporate an aquifer. The reservoir's projected lifespan is 20 years, with a fixed bottom hole pressure of 116 bar for each well. In the subsequent study focused on well placement optimization, the H-3B model will serve as the basis for analysis and experimentation.

Methodology

The detailed theory of the algorithms utilized in this research will be discussed in this section. Firstly, the WMPP method is introduced based on the DMPP method. And then, the objective function in the well placement optimization model is defined and analyzed. Finally, the specific workflow of simulated annealing algorithm for solving WMPP indexes is displayed.

Weighted mapping of productivity potential

The Direct Mapping of Productivity Potential (DMPP) is a valuable approach in reservoir engineering that enables a detailed understanding of the spatial variability in production potential. By integrating and analyzing diverse data types, DMPP helps in optimizing production strategies, enhancing recovery efficiency, making informed economic decisions, and managing risks effectively. The mathematic form of DMPP is given by:

$$J_{i,j,k}(t) = \left[S_{o,i,j,k}(t) - S_{or}\right] \cdot \left[p_{o,i,j,k}(t) - p_{min}\right] \cdot \ln(K_{i,j,k}) \cdot \ln(r_{i,j,k}) \cdot d_{woc,i,j,k} \cdot \phi_{i,j,k} \cdot d_{goc,i,j,k} \quad (1)$$

where, the subscript i, j, k is the index of gird block at x, y, z direction, respectively; $J_{i,j,k}(t)$ is the DMPP at gird block (i, j, k) at time t; $S_{o,i,j,k}(t)$ is the oil saturation at gird block (i, j, k) at time t; S_{or} is the residual saturation of oil at gird block (i, j, k); $p_{o,i,j,k}(t)$ is the oil pressure at gird block (i, j, k) at time t; p_{min} is the minimum well bottomhole pressure; $K_{i,j,k}$ is the permeability at gird block (i, j, k); $r_{i,j,k}$ is the distance from the gird block (i, j, k) to the closest boundary; $d_{woc,i,j,k}$ is the distance from the grid block (i, j, k) to the closest oil–water interface; $\phi_{i,j,k}$ is the porosity at the grid block (i, j, k); $d_{goc,i,j,k}$ is the distance from the grid block (i, j, k) to the closest gas-oil interface.

Literally, DMPP is a simple direct mapping ignoring reservoir backgrounds. While the DMPP offers a straightforward and generalized approach, it has limitations in adapting to diverse reservoirs with differing geological, physical characteristics, and production schedules. To address these limitations, the WMPP as an enhanced formulation is proposed in this study. The WMPP incorporates trainable weights into the workflow, allowing it to be customized to specific reservoir conditions. This flexibility makes the WMPP a valuable tool for characterization and management of versatile reservoirs.

Mathematically, the WMPP is expressed as Eq. (2), WMPP is a linear formulation of geological and physical properties with trainable weights in the given reservoir. These weights play a crucial role in tailoring the WMPP to the unique attributes of a given reservoir.

$$\begin{aligned} \mathrm{I_{i,j,k}(t)} = {} & \omega_1\left[\mathrm{S_{o,i,j,k}(t) - S_{or}}\right] + \omega_2\left[\mathrm{p_{o,i,j,k}(t) - p_{min}}\right] \\ & + \omega_3 \ln\left(\mathrm{K_{i,j,k}}\right) + \omega_4 \ln\left(\mathrm{r_{i,j,k}}\right) + \omega_5 \mathrm{d_{woc,i,j,k}} \\ & + \omega_6 \phi_{\mathrm{i,j,k}} + \omega_7 \mathrm{d_{goc,i,j,k}} \end{aligned} \quad (2)$$

and let:

$$\omega = [\omega_1, \omega_2, \ldots, \omega_7] \quad (3)$$

where $I_{i,j,k}(t)$ is the WMPP at position (i, j, k) at time t; $\boldsymbol{\omega}$ is a row vector of weights of corresponding variables, and the weight vector could be solved by optimization algorithms.

To ensure consistent and standardized data representation, the data of the seven geological and physical parameters are normalized using the min–max rule, as described in Eq. (4). Henceforth, if not specified, all the seven items in the Eq. (2) are normalized using min–max rule respectively:

$$\widetilde{x} = (x - x_{min})/(x_{max} - x_{min}) \quad (4)$$

where, x is the original value of data;

In practice, when considering a reservoir at a specific time t and applying the min–max rule, the WMPP formulation can be further simplified to following:

$$\mathrm{WMPP}_g = \omega x_g \quad (5)$$

where g is the grid block index, i.e.(i, j, k); WMPP_g is the WMPP at grid block numbered as g and x_g is a column vector composed of the seven parameters, i.e.$[S_g - S_{or}, p_g - p_{min}, \ln K_g, \ln r_g, d_{woc,g}, \phi_g, d_{goc,g}]$.

Objective function

Practically, reservoir simulations provide cumulative production data for wells rather than individual grid blocks. To align these simulations with the WMPP, we consider distributed wells on the reservoir plan map as probes for WMPP and cumulative production. Subsequently, we use reservoir simulation to obtain probing results, which serve as training data. Distributed wells on reservoir plan map can be deemed as probes of WMPP and cumulative production. And with reservoir simulation, the probing results was obtained and used as training data.

In line with the reservoir model described in Sect. "Model description", we generated random well locations, totaling 929 wells, while adhering to a minimum well spacing constraint. All 929 wells were fully perforated from top to

bottom across all reservoir layers. As previously mentioned, each well acts as a probe, and it's preferable to minimize well interference to enhance probing accuracy. Ideally, we would perform 929 simulations, each involving the drilling of a single well in the reservoir. However, such an approach would be excessively time-consuming and costly.

To strike a balance, we divided the 929 wells into 19 groups, as illustrated in Fig. 2. This division was made with the goal of reducing well interference as much as possible, considering the well spacing limit. Each group represented a case of well placement, and reservoir simulations were conducted to calculate cumulative productions over a specified period, such as 20 years in this demonstration.

The results from these 19 cases of reservoir simulations provided data on the cumulative production of single wells (Fig. 2b).

In essence, the productivity potential at a specific grid is expected to reflect the cumulative production of wells located at relevant positions. However, each well penetrates multiple grid blocks within the reservoir model, and different wells may traverse varying numbers of grids. It can be inferred that, for a single well, the more grids it traverses, the higher its cumulative production will be over a given period, as it has access to a larger potential flow area.

To account for this variation, we normalize the WMPP by considering the grid blocks that wellbores pass through. In this paper, we chose to average the WMPP values for grids neighboring a wellbore, as illustrated in Fig. 3. These selected grids, together with the wellbore, form a cylinder referred to as a "well cut".

Taking the well cuts as grid indices, we calculated the WMPP for each well by averaging the WMPP values of grids indexed within its associated well cut. This calculation is expressed as:

$$\mathrm{WMPP}_w(\omega) = \omega\left(\frac{\sum_{g_{w,n=1}}^{g_{w,N}} x_{g_{w,n}}}{g_{w,N}}\right) \tag{6}$$

where, $\mathrm{WMPP}_w(\omega)$ is the WMPP of well w; $g_{w,N}$ is the total number of grids of in the well cut of well w; $g_{w,n}$ is the grid numbered n within the well cut of well w;.

Let WOPT_w is the Well Oil Total Production (WOPT) of well w. At this point, we have a matrix composed of 929 tuples of (WMPP_w, WOPT_w), with each tuple serving as the basic sample unit in this paper.

Our objective is to find an optimized vector of weights i.e. ω, which results in wells with higher WMPP_w generally having higher WOPT_w, and vice versa. An ideal

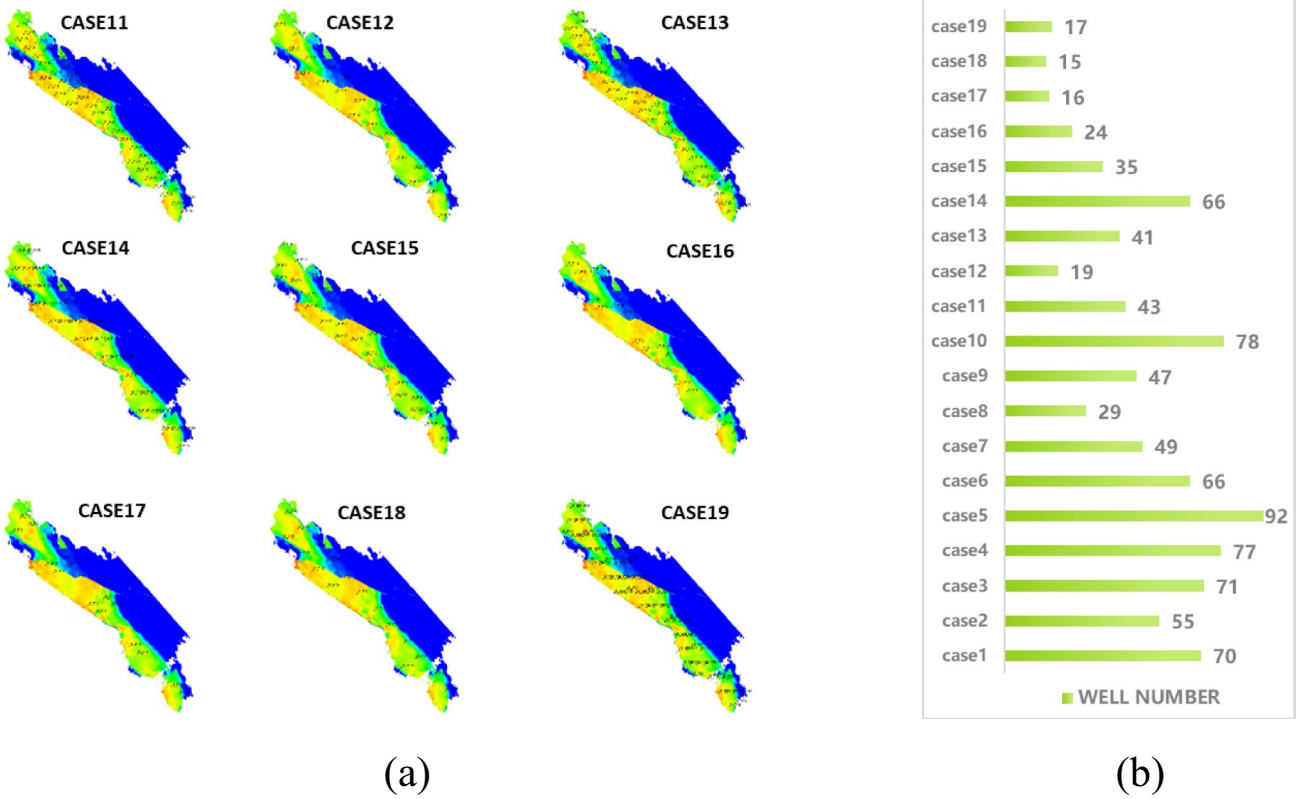

Fig. 2 Well Placement and numbers of random divided groups (case1-19) (**a** map of oil saturation and well placement of CASE11-19; **b** well numbers of case1-19)

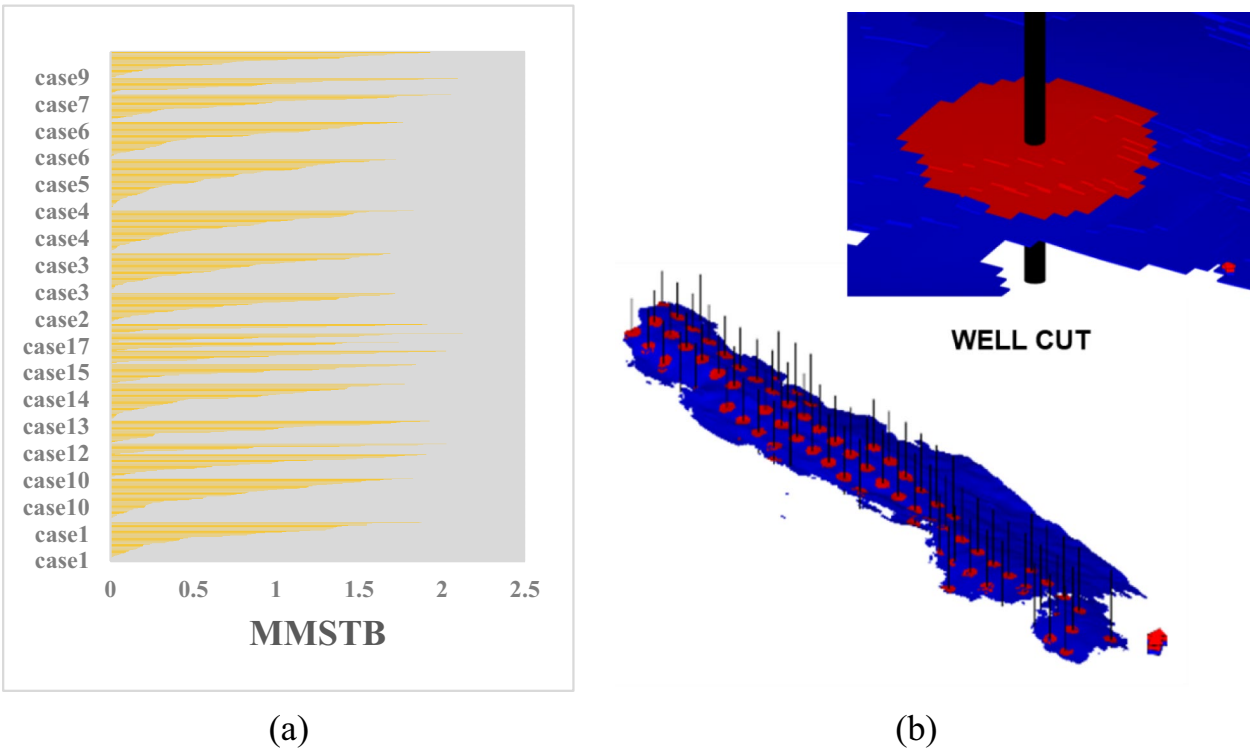

Fig. 3 Schematic of cumulative production of each cases and well cuts (**a** cumulative production of each cases; **b** schematic of well cut)

scenario would involve a perfect monotonic positive relationship between them. However, it's important to note that $WMPP_w$ is a linear formulation based on geological and physical parameters, while $WOPT_w$ are obtained through reservoir simulation involving complex and nonlinear function. Obviously, predicting future well production based solely on the seven parameters is challenging and almost impossible.

Therefore, our goal in this paper is not to directly regress the $WOPT_w$ using those parameters although an intricate function between $WMPP_w$ and $WOPT_w$ does exists. Instead, we employ the Spearman Rank Correlation Coefficient to represent this relationship in a more flexible manner.

The Spearman Rank Correlation Coefficient, developed by Charles Spearman in the early twentieth century, is a statistical measure utilized to assess the strength and direction of the monotonic relationship between two variables. This coefficient is particularly well-suited for cases where the relationship between variables is not linear but can be described by a consistent order or ranking, which exactly fits the problem. It quantifies the degree to which the variables tend to increase or decrease together in rank order and ranges from − 1 to 1, with negative values denoting a negative relationship, positive values indicating a positive relationship, and zero representing no correlation.

Given two variables $WMPP_w$ and $WOPT_w$, Spearman Rank Correlation Coefficient is formulated as:

$$\rho(\mathrm{WMPP}_w, \mathrm{WOPT}_w) = \frac{\mathrm{cov}\left(\mathrm{R}\left(\mathrm{WMPP}_w\right), \mathrm{R}\left(\mathrm{WOPT}_w\right)\right)}{\sigma\left(\mathrm{WMPP}_w\right)\sigma\left(\mathrm{WOPT}_w\right)} \tag{7}$$

where ρ represents the Spearman Rank Correlation Coefficient; and $\mathrm{R}\left(\mathrm{WMPP}_w\right)$ and $\mathrm{R}\left(\mathrm{WPT}_w\right)$ are converted rank variables of $WMPP_w$ and WPT_w, respectively; $\sigma(\cdot)$ and $\mathrm{cov}(\cdot)$ are standard deviation and covariance, respectively.

To conclude, the mathematical problem in our case is formulated as:

$$\omega^* = \mathrm{argmax}\left(\frac{\mathrm{cov}\left(\mathrm{R}\left(\mathrm{WMPP}_w\right), \mathrm{R}\left(\mathrm{WOPT}_w\right)\right)}{\sigma\left(\mathrm{WMPP}_w\right)\sigma\left(\mathrm{WOPT}_w\right)}\right) \tag{8}$$

where ω^* is the most optimized ω that maximizes the Spearman Coefficient between WMPP and WPT of wells.

The optimization objective is defined as the Spearman correlation coefficient between the Single-Well WMPP and WOPT. Through multiple random cases and numerical simulations, it is ensured that the established WMPP exhibits a statistically significant positive correlation with WOPT. This offers reservoir engineers stable and reliable reference data for well placement decisions.

The following sections of this paper will detail the methodology for acquiring the optimized vector of weights ω^* using a simulated annealing algorithm.

Solve WMPP using simulated anneal algorithm

Overall approach for WMPP calculation

Based on reservoir numerical simulation results and optimization algorithm, WMPP tailored to a specific oilfield is developed by integrating spatial properties such as porosity, permeability, oil saturation, and the position of the oil–water interface. WPMM provides direct and effective guidance for well placement within the oilfield. By computing the weighted average of spatial properties in the vicinity of well locations, the average spatial attributes of well placements are characterized. This approach considers the highly complex non-linear relationship between the average spatial attributes of well locations and cumulative production. The technical workflow for calculating the WMPP is illustrated in Fig. 4. It primarily involves multiple numerical simulations for random well locations, computation of average attributes in the vicinity of all well locations, and optimization of attribute weights using the simulated annealing (SA) algorithm.

Simulated annealing algorithm

Simulated annealing (SA) is a powerful optimization algorithm rooted in statistical mechanics and the concept of annealing in metallurgy. At its core, it's designed to find the optimal solution of a complex problem by mimicking the annealing process where a material is slowly cooled to reach its lowest energy state. It is particularly effective for solving complex optimization problems, such as ours, where traditional gradient-based methods may struggle due to the nonlinear and intricate nature of the relationships involved.

The simulated annealing algorithm begins with an initial solution and iteratively explores the solution space, allowing it to escape local optima and converge towards a global optimum. This exploration process involves accepting new solutions based on a probabilistic criterion, which allows the algorithm to explore different areas of the solution space while avoiding premature convergence. The following is the details of the SA algorithm.

1. Exploration Space

$$S = \{[\omega_1, \omega_2, \ldots, \omega_7] | \omega_m \in [0,1], m = 1,2, \ldots, 7\} \quad (9)$$

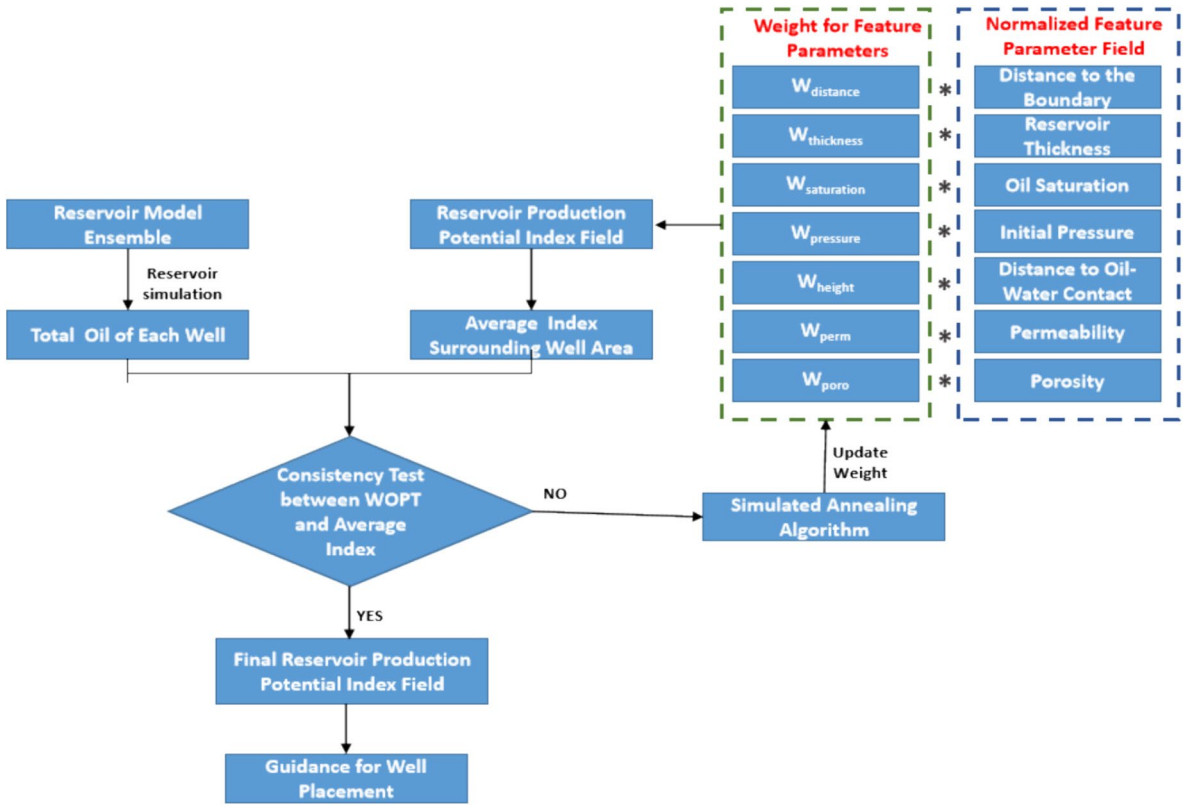

Fig. 4 The specific workflow for calculating the WMPP indexes

The search space S of weights of WMPP is shown in Eq. (9). Initial solution is needed for simulated annealing. Since each weight represents relative importance of its corresponding parameter, $\omega = [0.5,0.5,\ldots,0.5]$ is defined as the initial solution, aligning the same weight for each.

2. Objective Function

In our scenario, the objective is to find the optimal vector of weights of WMPP that maximizes the Spearman Rank Correlation Coefficient between WMPP and WPT.

3. Neighbor Generation

At each iteration, a neighboring solution is generated by perturbing the current solution. This perturbation can be thought of as a small change in the weights, similar to the thermal fluctuations in a material during annealing. The new solution can be expressed as:

$$\omega_{new,m} = \begin{cases} 0, \omega_{old,m} + \Delta\omega_m < 0 \\ \omega_{old,m} + \Delta\omega_m, 0 \le \omega_{old,m} + \Delta\omega_m \le 1 \\ 1, 1 < \omega_{old,m} + \Delta\omega_m \end{cases} \quad (10)$$

where $\omega_{new,m}$, $\omega_{old,m}$, $\Delta\omega_m$ is the new solution, current solution, small change in solution of a specific weight numbered m in $\boldsymbol{\omega}$. To achieve moderate and balanced random search in SA algorithm, and effectively explore the solution space without excessive jumping or getting stuck in local optima $\Delta\omega_m$ is sampled from a normal distribution with standard error of 0.06 and mean of 0.

4. Acceptance Criterion: Metropolis–Hastings Criterion

The acceptance of a new solution is determined by the Metropolis-Hastings criterion, which is a fundamental aspect of the simulated annealing algorithm. It involves the following mathematical expression:

$$P_{accept} = \begin{cases} min\left(1, e^{-\frac{\Delta E}{T_{old}}}\right), & \Delta E \ge 0 \\ 1, & \Delta E < 0 \end{cases} \quad (11)$$

where: P_{accept} is the probability of accepting the new solution; T_{old} is the current temperature; ΔE is the change in the objective function between the current solution and new solution (in our scenario, the change in Spearman Coefficient, i.e. $\Delta E = \rho\left(WMPP\left(\omega_{old}\right), WPT\right) - \rho\left(WMPP\left(\omega_{new}\right), WPT\right)$.

This criterion embodies the probabilistic nature of the algorithm. If the neighboring solution improves the objective function ($\Delta E < 0$), it is always accepted ($P_{accept} = 1$). However, if the new solution is worse ($\Delta E < 0$), it is accepted with a decreasing probability as the temperature decreases. This probabilistic acceptance allows the algorithm to explore the solution space systematically and escape local optima.

5. Temperature Annealing

As mentioned, simulated annealing uses a temperature parameter T that controls the probability of accepting new solutions. Initially, T is set high, which means that we are more willing to accept worse solutions to explore the solution space broadly. Over iterations, T decreases, mimicking the cooling process. The temperature reduction is often done as following:

$$T_{new} = \alpha T_{old} \quad (12)$$

where: T_{new} is the new temperature; T_{old} is the current temperature; α is the cooling factor. According to the experience in the previous study (Bertsimas and Tsitsiklis 1993), α is set as 0.99 in this research.

6. Iterating until termination

Repeat steps (3), (4), (5) until the process meets its termination condition: the temperature reaches the predefined threshold (Tend = e-20). The final solution represents the optimized weights that maximize the Spearman Rank Correlation Coefficient.

The optimization process performed 866 iterations and came to a plateau of Spearman coefficient of 0.873. During the iterations, especially at the early periods, the object function (Spearman coefficient) fluctuates violently, indicating the acceptance of worse objects to expand the search range to escape local optimum as shown in Fig. 5.

Finally, the spearman coefficient reaches its maximum of 0.873 (Fig. 5), with corresponding weights given by:

$$w = [0.18,0.83,0,83,0.16,0.43,0.13,0.46] \quad (13)$$

Thus, the WMPP is:

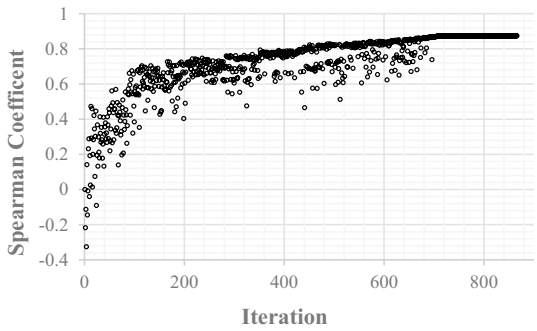

Fig. 5 The detailed Spearman coefficient evolution with iterations

$$
\begin{aligned}
WMPP_{i,j,k} = {} & 0.18\left(S_{i,j,k} - S_{or}\right) + 0.83\left(P_{i,j,k} - P_{min}\right) \\
& + 0.83 \ln K_{i,j,k} + 0.16 \ln r_{i,j,k} \\
& + 0.43 d_{woc,i,j,k} + 0.13 \Phi_{i,j,k} \\
& + 0.46 d_{goc,i,j,k}
\end{aligned} \tag{14}
$$

According to the Eq. (14), the WMPP mapped on all grids of the reservoir is shown in Fig. 6.

Results and discussion

In this section, by conducting a comprehensive examination and analysis of the consistency between WOPT and the wellbore weighted mapping of productivity potential (WMPP) for the H-3B model across 19 optimization cases, the weighting factors are obtained.

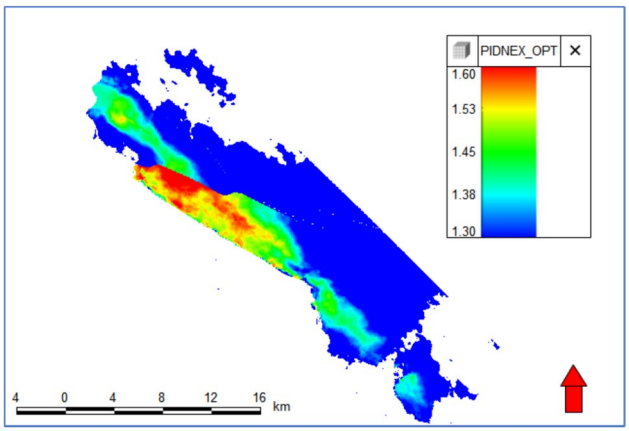

Fig. 6 The WMPP map of the H-3B reservoir (the bold red arrow points in the direction of north, the red-yellow patches represent the WMPP indexes)

Subsequently, a test case (CASE20) is established to evaluate the alignment of the WOPT with wellbore WMPP, direct mapping of productivity potential (DMPP), and oil initially in place (OOIP). And then, a holistic comparative analysis encompassing 20 different cases is conducted. It is worth mentioning that the Spearman correlation coefficients between WOPT, various attributes of wellbores, and WMPP and DMPP are assessed. This comprehensive assessment serves to validate the applicability and reliability of the methodology developed in this study. Finally, the obtained WMPP is applied in the deployment of horizontal wells in the H-3B reservoir, achieving favorable results. This demonstrates that WMPP is not only suitable for guiding vertical well placement but also proves to be effective in guiding the deployment of horizontal wells.

Adaptability analysis of WMPP

In Sect. "Objective function", statistical graphs for each of the 19 training sample cases are presented, displaying both WOPT and the average wellbore WMPP calculated based on the well cut. As shown in Fig. 7, this graph illustrates a notable and robust correlation within the training samples between WOPT and WMPP in the vicinity of the well.

The Spearman correlation coefficients between single-well WOPT and WMPP for the 19 cases are illustrated in Fig. 8. The smallest correlation coefficient, corresponding to CASE12, is 0.78, with an average coefficient of 0.85. This indicates that the WMPP field obtained after optimization of weighting factors provides effective guidance for well placement to maximize cumulative oil production.

In Fig. 8, the Spearman correlation coefficients between WOPT and various attribute variables (thickness, distance to boundary (DOB), distance to water contact (DOWC), initial pressure (INIPRESS), WMPP (PINDEX_OPT)), as

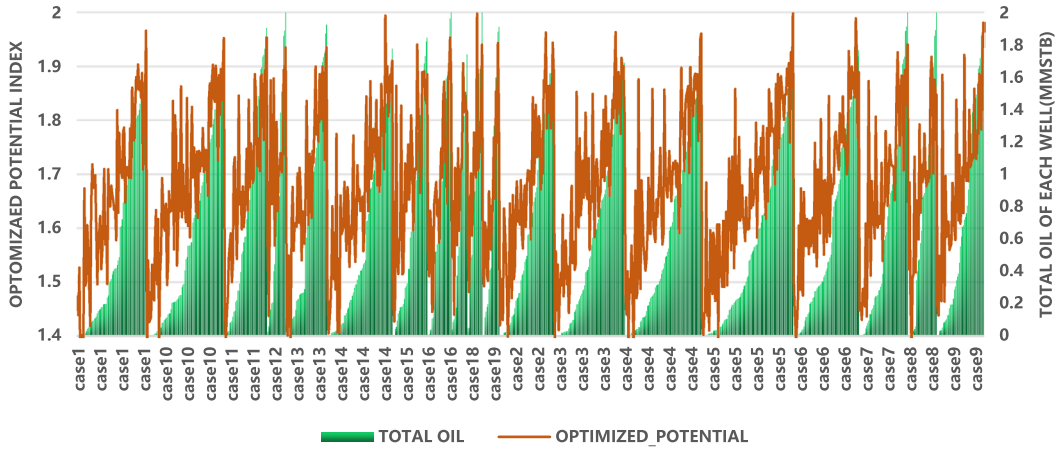

Fig. 7 WMPP and WOPT of wells in all the studied cases

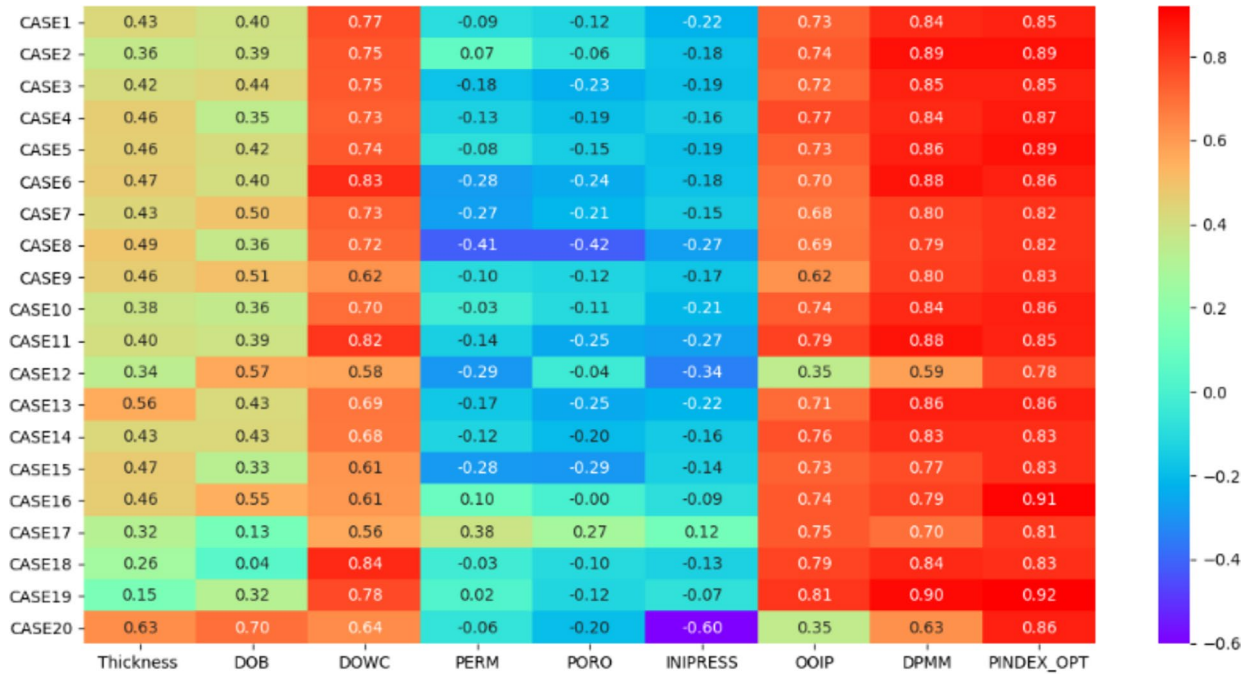

Fig. 8 Heat map of Spearman correlations between WOPT and various attribute variables, as well as DMPP and WMPP in twenty cases

well as DMPP and WMPP, are presented for all cases concerning the H-3B model. It is evident that, for the H-3B model, WMPP exhibits a strong positive correlation with WOPT in all cases. This indicates that WMPP can effectively guide well placement optimization to maximize the cumulative oil production of individual wells. Furthermore, DMPP, OOIP, and DOWC also play a role in guiding well placement optimization concerning single-well cumulative oil production, although their effectiveness is slightly inferior to WMPP. Specifically, the hierarchy of their influence is WMPP > DMPP > DOWC > OOIP. Additionally, PERM (permeability), PORO (porosity), and INIPRESS (initial pressure) show a certain negative correlation with single-well cumulative oil production, indicating a negative relationship between these attribute variables and the cumulative oil production of individual wells.

Furthermore, a test case (CASE20) which encompassing a total of 18 production wells is established to validate the reliability of the WMPP method. The distribution of well placements and the WMPP obtained through optimization are depicted in Fig. 9. These test cases adhere to the same well operation regime as the training cases. The final cumulative oil production falls within the range of 0.05 to 2.0 million stock tank barrels (MMSTB), demonstrating a relatively uniform distribution.

In the test case (18 wells), the Spearman correlation coefficient between WOPT and the WMPP are examined and shown in Fig. 10. Wells 20_P2, 20_P3, 20_P15, 20_P5, 20_P6, and 20_P1 have higher WMPP in their respective

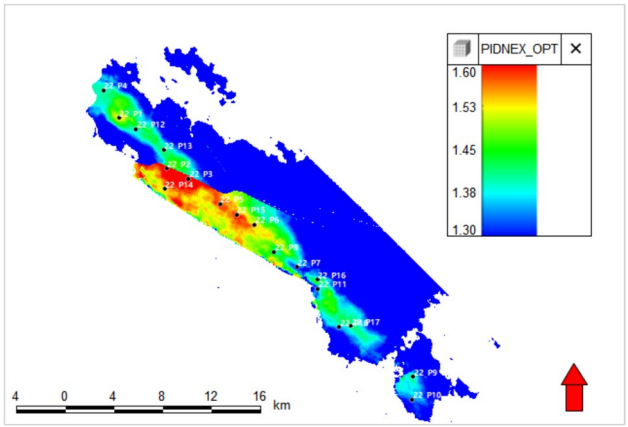

Fig. 9 Well placement and WMPP distribution of case 20 (the bold red arrow points in the direction of north)

regions. These wells also exhibit relatively higher WOPT. Among them, wells 20_P2 and 20_P3 have the highest average WMPP within their vicinity. However, the WOPT of these two wells is lower than that of well 20_P15. This is because wells 20_P2 and 20_P3 are located too close to a sealed fault, and the distance to the fault was not considered in the calculation of WMPP. Wells 20_P11, 20_P7, 20_P10, 20_P9, and 20_P16 have lower WMPP in their respective regions, and these wells also exhibit relatively lower cumulative oil production.

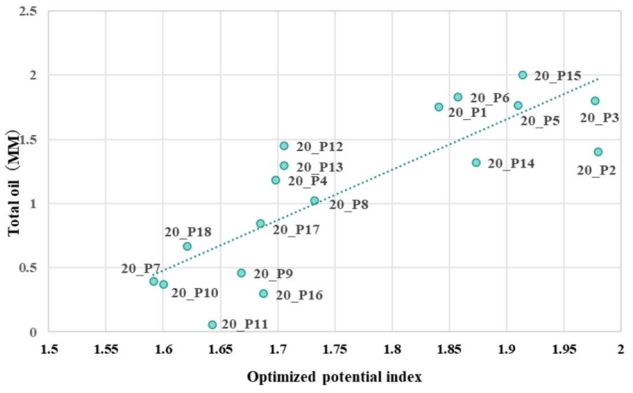

Fig. 10 The Spearman correlation coefficient between WOPT and the WMPP of wells in case20

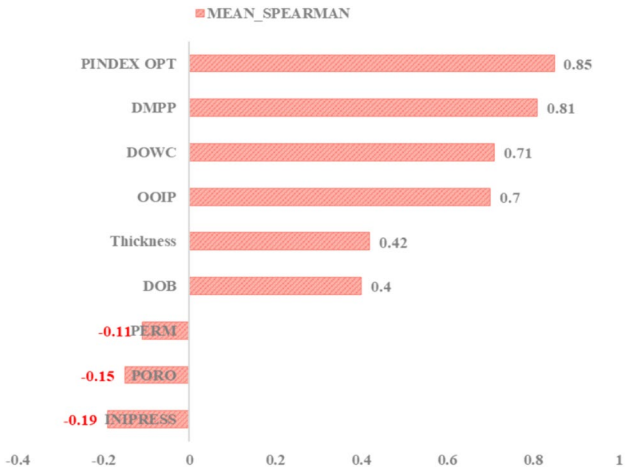

Fig. 11 Mean Spearman correlations between WOPT and various attribute variables, as well as DMPP and WMPP among twenty cases (the red letters mean negative number)

Guiding well placement based on OOIP is currently one of the primary methods in field development. Figure 8. also provides a visual representation of the comparison for all 20 cases. It is evident that the WMPP established in this study outperforms OOIP-guided well placement, demonstrating a significant advantage. Furthermore, compared to the DMPP method mentioned in the literature, the application of WMPP shows notable improvements in performance across the board, particularly in the case of CASE12 and CASE20. In Fig. 11, the statistics of the average Spearman correlation coefficients between WMPP, DMPP, various attribute values, and WPOT across the 20 cases. Importantly, WMPP demonstrates a 4.9% improvement in correlation compared to DMPP and a substantial 21.4% increase compared to OOIP.

Field application for horizontal well placement

Furthermore, the obtained WMPP is utilized in the design of horizontal well placement schemes for the H-3B reservoir. In the plan view, regions with relatively high WMPP values are selected, while the trajectories of the horizontal wells are adjusted based on the magnitude of WMPP values on the well placement profiles. This adjustment aimed to guide the well trajectories through areas with larger WMPP values whenever possible. The horizontal well placement scheme for the H-3B reservoir based on WMPP is illustrated in Fig. 12 and Fig. 13 present the optimization results of the well trajectories for PROFILE1 and PROFILE2 horizontal wells, guided by WMPP.

A comparison study between two well placement schemes using Eclipse reservoir numerical simulation software are conducted. The first scheme involved the placement of 105 wells guided by WMPP, while the second scheme consisted of 112 wells placed based on OOIP guidance. Both sets of schemes utilized identical injection and production control parameters, with oil wells set to maintain a constant bottom-hole pressure of 116 bar and an injection-to-production ratio of 1 throughout the reservoir. The simulations were run for a 20-year production period. The total oil production of the WMPP method is 147.35 million stock tank barrels (MMSTB) with the number of 105 wells, while that of the OOIP method is 128.9 MMSTB with the number of 112 wells. It is evident that the well placement scheme guided by WMPP, which required 7 fewer wells than the OOIP-based scheme, resulted in a remarkable increase in field total oil production (FTOP) over the 20-year period. Specifically, the total cumulative oil production increased by 18.45 MMSTB, and the average cumulative oil production per well rose from 1.15 MMSTB to 1.40 MMSTB, representing a 21.74% improvement. This outcome demonstrates a significant positive impact of the WMPP-guided approach.

Conclusions

1. Through the development and application of the SA algorithm, the optimized weighting coefficients for WMPP were determined for maximizing the Spearman Rank Correlation Coefficient between WMPP and well oil total production (WOPT).
2. The well placement scheme obtained by WMPP, which required 7 fewer wells than the oil initially in place (OOIP)-based scheme, improved 21.74% oil production over the twenty years production period.
3. Comparative analyses revealed that WMPP outperforms traditional methods, including DMPP and OOIP, indicating its superior efficacy in guiding well placement strategies.

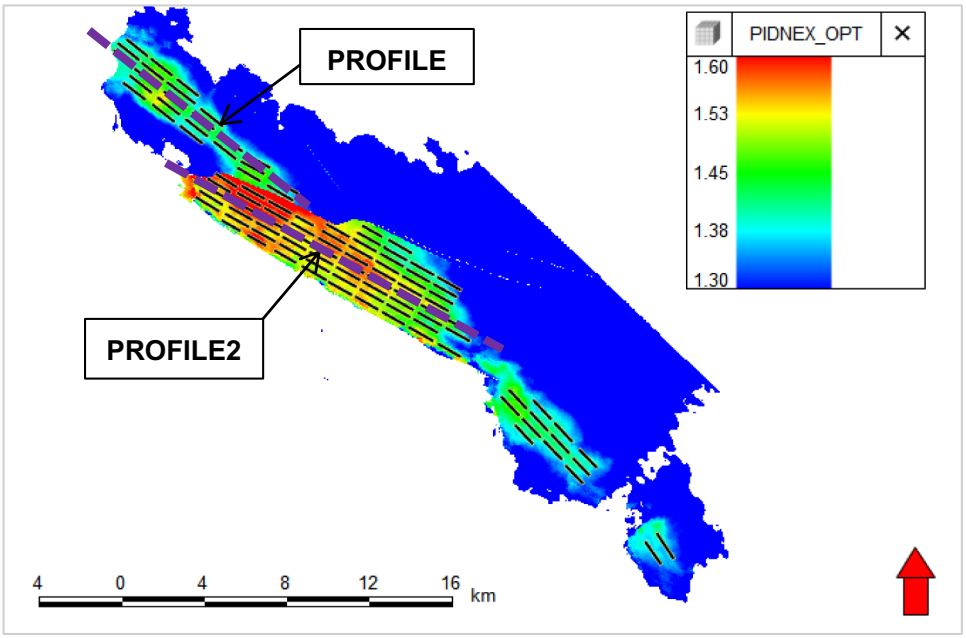

Fig. 12 Placement of horizontal wells based on WMPP method in the H-3B reservoir

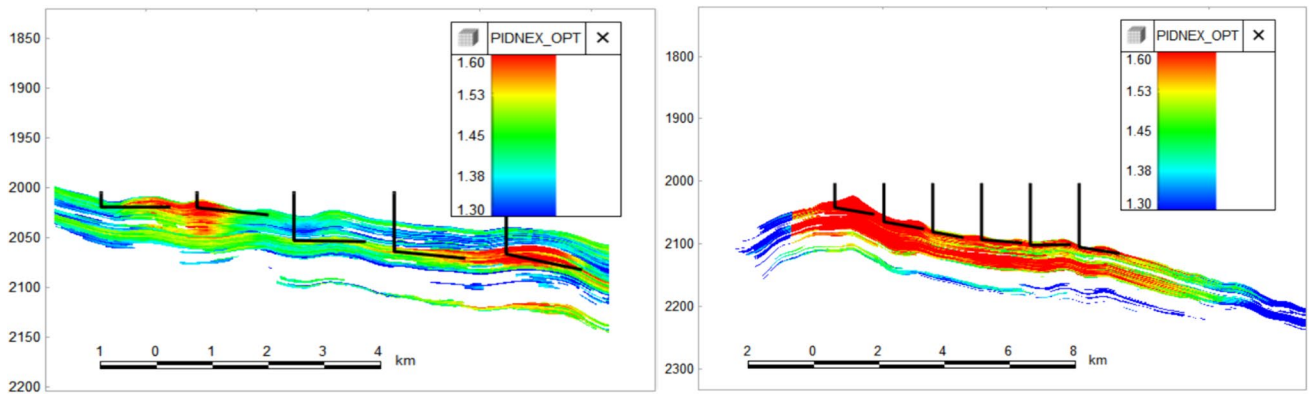

Fig. 13 Well trajectories of horizontal wells instructed by WMPP method in the H-3B reservoir

4. The WMPP-guided well placement scheme not only reduced the number of wells required but also enhanced the average cumulative oil production per well, underscoring the economic and operational benefits of this approach.

Acknowledgements This research was supported by the Fundamental Innovation Team Support Project titled "Evaluation of Porous Carbonate Reservoirs and Fundamental Research on Waterflooding Simulation" (J2301), and the scientific research topic "Integrated Data-Driven and Spatio-Temporal Simulation Inversion for Complex Carbonate Reservoir Production Development Strategies" (R2302).

Author contributions Rui Deng: Writing—original draft preparation, Conceptualization, Methodology, Formal analysis and investigation. Bo Kang: Conceptualization, Formal analysis and investigation. Liang Zhang: Conceptualization, Formal analysis and investigation, Writing—review and editing, Funding acquisition. Lian Wang: Methodology, Writing—review and editing. Bing Xu: Methodology. Xing Zhao: Writing—review and editing. Ce Duan: Writing—original draft preparation.

Funding Fundamental Innovation Team Support Project, J2301, Liang Zhang, R2302, Liang Zhang.

Data Availability Data will be made available on request.

Declarations

Conflict of interest The authors declare that they have no conflict of interest.

References

Akin S, Kok MV, Uraz I (2010) Optimization of well placement geothermal reservoirs using artificial intelligence. Comput Geosci 36(6):776–785. https://doi.org/10.1016/j.cageo.2009.11.006

Algosayir MM (2012) Optimization of Steam/Solvent Injection Methods: Application of Hybrid Techniques with Improved Algorithm Configuration. https://doi.org/10.7939/R3513W

Azamipour V, Assareh M, Eshraghi R (2023) Development of an effective completion schedule for a petroleum reservoir with strong aquifer to control water production. J Petrol Explor Prod Tech 13(1):365–380. https://doi.org/10.1007/s13202-022-01555-5

Badru O, Kabir CS (2003) Well placement optimization in field development. In: SPE Annual Technical Conference and Exhibition. Society of Petroleum Engineers, SPE-84191-MS. https://doi.org/10.2118/84191-MS

Bangerth W, Klie H, Wheeler MF (2006) On optimization algorithms for the reservoir oil well placement problem. Comput Geosci 10(3):303–319. https://doi.org/10.1007/s10596-006-9025-7

Baouche R, Wood DA (2020) Characterization and estimation of gas-bearing properties of Devonian coals using well log data from five Illizi Basin wells (Algeria). Adv Geo-Energy Res 4(4):356–371. https://doi.org/10.46690/ager.2020.04.03

Bellout MC, Volkov O (2018) Development Of efficient constraint-handling approaches for well placement optimization. ECMOR XVI—16th European Conference on the Mathematics of Oil Recovery. https://doi.org/10.3997/2214-4609.201802247

Bertsimas D, Tsitsiklis J (1993) Simulated annealing. Stat Sci 8(1):10–15. https://doi.org/10.1214/ss/1177011077

Bouzarkouna Z, Ding DY, Auger, (2012) Well placement optimization with the covariance matrix adaptation evolution strategy and meta-models[J]. Comput Geosci 16(1):75–92. https://doi.org/10.1007/s10596-011-9254-2

Ding S, Jiang H, Li J, Tang G (2014) Optimization of well placement by combination of a modified particle swarm optimization algorithm and quality map method. Comput Geosci 18(5):747–762. https://doi.org/10.1007/s10596-014-9422-2

Ghassemzadeh S, Perdomo MG, Haghigh M (2019) Application of deep learning in reservoir simulation. Petrol Geostat. https://doi.org/10.3997/2214-4609.201902252

Guyaguler B (2002) Optimization of Well Placement and Assessment of Uncertainty. Stanford University, 3048536.

Humphries TD, Haynes (2015) Joint optimization of well placement and control for nonconventional well types. J Petrol Sci Eng 126:242–253. https://doi.org/10.1016/j.petrol.2014.12.016

Leeuwenburgh O, Egberts PJP, Abbink OA (2010) Ensemble methods for reservoir life-cycle optimization and well placement. In: SPE/DGS Saudi Arabia Section Technical Symposium and Exhibition. Society of Petroleum Engineers, SPE-136916-MS. https://doi.org/10.2118/136916-MS

Liu N, Jalali Y (2006) Closing the loop between reservoir modeling and well placement and positioning. In: SPE Intelligent Energy International Conference and Exhibition. SPE-98198-MS. https://doi.org/10.2118/98198-MS

Olabode O, Isehunwa S, Orodu O (2021) Optimizing productivity in oil rims: simulation studies on horizontal well placement under simultaneous oil and gas production. J Petrol Explor Prod 11(1):385–397. https://doi.org/10.1007/s13202-020-01018-9

Portella RCM, Hewett TA (2000) Upscaling, gridding, and simulating using streamtubes. Spe J 5(3):315–323. https://doi.org/10.2118/65684-PA

Rostamian A, de Sousa MMV, Mirzaei-Paiaman A (2024) Analysis of different objective functions in petroleum field development optimization. J Petrol Explor Prod Technol 2024:1–21. https://doi.org/10.1007/s13202-024-01848-x

Sobhi I, Dobbi A, Hachana O (2022) Prediction and analysis of penetration rate in drilling operation using deterministic and metaheuristic optimization methods. J Petrol Explor Prod Technol 12(5):1341–1352. https://doi.org/10.1007/s13202-021-01394-w

Syed FI, Negahban S (2021) Dahaghi A K (2021) Infill drilling and well placement assessment for a multi-layered heterogeneous reservoir. J Petrol Explor Prod 11:901–910. https://doi.org/10.1007/s13202-020-01067-0

Thenon A, Gervais V, Ravalec ML (2016) Multi-fidelity proxy models for reservoir engineering. ECMOR XV—15th European Conference on the Mathematics of Oil Recovery. https://doi.org/10.3997/2214-4609.201601831

Wang L, Li ZP, Adenutsi CD (2021) A novel multi-objective optimization method for well control parameters based on PSO-LSSVR proxy model and NSGA-II algorithm. J Petrol Sci Eng 196:107694. https://doi.org/10.1016/j.petrol.2020.107694

Wang L, Yao Y, Zhang T (2022) A novel self-adaptive multi-fidelity surrogate-assisted multi-objective evolutionary algorithm for simulation-based production optimization. J Petrol Sci Eng 211:110111. https://doi.org/10.1016/j.petrol.2022.110111

Wang L, Yao Y, Luo X (2023) A critical review on intelligent optimization algorithms and surrogate models for conventional and unconventional reservoir production optimization. Fuel 350:128826. https://doi.org/10.1016/j.fuel.2023.128826

Wood DA, Choubineh A (2019) Reliable predictions of oil formation volume factor based on transparent and auditable machine learning approaches. Adv Geo-Energy Res 3(3):225–241. https://doi.org/10.26804/ager.2019.03.01

Yavari H, Khosravanian R, Wood DA (2021) Application of mathematical and machine learning models to predict differential pressure of autonomous downhole inflow control devices. Adv Geo-Energy Res 5(4):386–406. https://doi.org/10.46690/ager.2021.04.05

Yeten B, Durlofsky LJ, Aziz K (2003) Optimization of nonconventional well type, location, and trajectory. Spe J 8(3):44–53. https://doi.org/10.2118/86880-PA